Genomic Signatures Define Three Subtypes of *EGFR*-Mutant Stage II-III NSCLC With Distinct Adjuvant Therapy Outcomes

Si-Yang Liu
Guangdong Lung Cancer Institute, Guangdong Provincial People's Hospital, and Guangdong Academy of Medical Sciences, School of Medicine, South China University of Technology

Hua Bao
Geneseeq Technology Inc.

Qun Wang
Department of Thoracic Surgery, Zhongshan Hospital, Fudan University

Weimin Mao
Zhejiang Cancer Hospital

Yedan Chen
Nanjing Geneseeq Technology Inc.

Xiaoling Tong

Song-Tao Xu
Fudan University Affiliated Zhongshan Hospital

Lin Wu
Departments of Thoracic Medicine, Hunan Cancer Hospital

Yu-Cheng Wei
The Affiliated Hospital of Medical College Qingdao University

Yong-Yu Liu
Shenyang Chest Hospital

Chun Chen
Fujian Medical University Union Hospital

Ying Cheng
Jilin Provincial Tumor Hospital

Rong Yin
Nanjing Medical University https://orcid.org/0000-0002-9744-4251

Fan Yang
Peking University People's Hospital

Shengxiang Ren
Shanghai pulmonary hospital, Tongji University

Xiao-Fei Li

Tangdu Hospital

Jian Li

Peking University First Hospital

Cheng Huang

Fujian Cancer Hospital

Zhidong Liu

Capital Medical University

Shun Xu

The First Hospital of China Medical University

Ke-Neng Chen

Department of Thoracic Surgical Oncology, Beijing Cancer Hospital

Shi-Dong Xu

Harbin Medical University Cancer Hospital

Lunxu Liu

West China Hospital of Sichuan University https://orcid.org/0000-0003-3964-5378

Ping Yu

Sichuan Cancer Hospital

Bu-Hai Wang

The Northern Jiangsu People's Hospital

Haitao Ma

The First Affiliated Hospital of Soochow University

Hong-hong Yan

Guangdong Provincial People's Hospital

Song Dong

Guangdong Provincial People's Hospital

Xu-Chao Zhang

Guangdong Academy of Medical Sciences, Guangzhou 510080

Jian Su

Guangdong Provincial People's Hospital

Jin-Ji Yang

Guangdong Lung Cancer Institute, Guangdong Provincial People's Hospital, and Guangdong Academy of Medical Sciences, School of Medicine, South China University of Technology

Xue-Ning Yang

Guangdong Provincial People's Hospital

Qing Zhou

Guangdong Lung Cancer Institute, Guangdong Provincial People's Hospital, Guangdong Academy of Medical Sciences

Xue Wu

Translational Medicine Research Institute, Geneseeq Technology Inc. https://orcid.org/0000-0002-5567-1325

Yang Shao

Princess Margaret Cancer Centre

Wen-Zhao Zhong

Guangdong Provincial People's Hospital https://orcid.org/0000-0002-8917-8635

Yi-Long Wu (**syylwu@live.cn**)

Guangdong Lung Cancer Institute, Guangdong General Hospital, and Guangdong Academy of Medical Sciences https://orcid.org/0000-0002-3611-0258

Article

Keywords: Adjuvant therapy, EGFR, TKI, Chemotherapy, Non-small-cell lung Cancer

Posted Date: May 3rd, 2021

DOI: https://doi.org/10.21203/rs.3.rs-457070/v1

Version of Record: A version of this preprint was published at Nature Communications on November 8th, 2021. See the published version at https://doi.org/10.1038/s41467-021-26806-7.

Abstract

The ADJUVANT study reported the comparative superiority of adjuvant gefitinib over chemotherapy in disease-free survival (DFS) of resected EGFR-mutant stage II-IIIA non-small cell lung cancer (NSCLC). However, not all patients experienced favorable clinical outcomes with TKI, raising the necessity for further biomarker assessment. By comprehensive genomic profiling of 171 tumor tissues from the ADJUVANT trial, five predictive biomarkers were identified (TP53 exon4/5 mutations, RB1 alterations, and copy number gains of NKX2-1, CDK4, and MYC. Then we integrated them into the Multiple-gene INdex to Evaluate the Relative benefit of Various Adjuvant therapies (MINERVA) score, which categorized patients into three subgroups with relative disease-free survival and overall survival benefits from either adjuvant gefitinib or chemotherapy (Highly TKI-Preferable, TKI-Preferable, and Chemotherapy-Preferable groups). This study demonstrates that predictive genomic signatures could potentially stratify resected EGFR-mutant NSCLC patients and provide precise guidance towards future personalized adjuvant therapy.

Introduction

Cisplatin-based adjuvant chemotherapy currently constitutes the standard-of-care after curative surgery for stage IIA-IIIB resected non-small cell lung cancer (NSCLC) [1, 2]. However, the 5-year survival rate still remains unsatisfactory, with alarming levels of grade 3 toxicity observed in more than 60% of the patients [3]. Hence, alternative adjuvant regimens with epidermal growth factor receptor (EGFR) tyrosine kinase inhibitors (TKI) have been studied through several prospective trials [4, 5]. The randomized phase III ADJUVANT study has actually presented significant prolonged disease-free survival (DFS) in *EGFR*-mutant NSCLC, after adjuvant gefitinib, as compared to the DFS after chemotherapy with vinorelbine and cisplatin (VP) [6]. Two phase 2 trials, SELECT and EVAN, have shown improved 2-year DFS with erlotinib. Early revelations of the ADAURA trial also presented remarkable improvements of DFS with the third generation EGFR-TKI, osimertinib [7, 8, 9]. However, approximately 19% to 40% of TKI-treated patients still relapse after these trials [6, 7], suggesting the inadequacy of *EGFR*-sensitizing mutants alone as a biomarker for adjuvant treatment selection.

The mixed clinical responses of NSCLC with targeted therapy can be attributed to molecular heterogeneity caused by different clonal populations, aggregated in a particular tumor, undergoing stage-specific evolution. Resulting selective pressure then further induces subclonal mutations, and promotes tumor expansion [10, 11, 12 13] The most prevalent co-mutations, such as alterations in the *TP53*, *RB1* and *NKX2-1*, usually cooperate to promote a local growth advantage, and support clonal expansion throughout tumor development [10, 11, 15]. In advanced *EGFR* mutant NSCLC, tumors with concurrent *TP53* or *RB1* mutations then further disrupted genome stability and exerted higher risks for histological transformation and TKI resistance[16]. In addition to gene level alterations, co-mutations on the exon levels can also affect patient outcomes[17].

As early-stage NSCLC also shows a high degree of intratumor heterogeneity with divergent evolutionary lineages[14], the established norm of estimating only a single driver oncogene through randomized trials for adjuvant targeted therapies fails to address the underlying complications of intratumor molecular heterogeneity. In this regard, the development of next-generation sequencing (NGS) technology has accelerated the analysis and integration of huge bulks of genomic signatures, thereby increased the focus on developing multi-gene predictive models for therapeutic decisions[18, 19]. Currently, in most single-armed cohort studies, biomarkers were analyzed for their prognostic effects by comparing survival differences between mutant and wildtype patients. However, the more challenging question is whether these biomarkers result in distinct outcomes under different treatments to ultimately guide therapeutic decisions. Therefore, it is important to distinguish predictive markers from the prognostic ones at first. The frequently used term “predict the prognosis” in many biomarker studies may confuse readers of the accurate definition for these two types of biomarkers. Specifically, a predictive biomarker differentiates treatment-specific survival benefits in biomarker- positive or negative patients [20] and further improves patients’ treatment outcomes, while a prognostic biomarker discriminates good or poor survival of patients regardless of treatment. For example, aberrations in the tumor suppressor *TP53* gene are known to correlate with worse prognosis comparing to *TP53* wildtype cancers[17, 21].

Moreover, to reduce the complications in choosing the appropriate statistical tests, a standard and reliable analytical method has been endorsed by Rothwell [22] and applied in numerous studies [23, 24]. As suggested, testing subgroup-treatment effect interaction is a prerequisite in reporting the predictive significance other than subjective observations of the survival curves. Subsequently, a linear discriminant using summation of all predictive values over the set of selected biomarkers is usually adopted for composite score development [25].

Herein in this study, we conducted a thorough explorative analysis of cancer-related genes through NGS of tumor tissues from the *EGFR*-mutant patients of the ADJUVANT trial, in an attempt to address important co-mutations and identify key predictive biomarkers for adjuvant treatment. We also integrate them into a robust predictive score that can categorize patients into subgroups with distinct survival benefits under either adjuvant gefitinib, or chemotherapy for precision care.

Results

Identification of predictive biomarkers from differential DFS

171 patients from the ADJUVANT trial with available baseline surgical specimens have been enrolled for genomic profiling (Fig. 1). The basic characteristics of the patients included in this exploratory cohort have been summarized in Supplementary Table 1. Comprehensive genomic profiling of 422 cancer-related genes revealed comparable frequencies of the highest mutated genes between the two treatment groups (Supplementary Fig. 1). *EGFR* 19del (49% vs. 45%), L858R (47% vs. 53%), and copy number gain (CN gain, 17% vs. 26%) were equally distributed in the adjuvant gefitinib and VP groups. Other co-mutations, including *TP53* (70% vs 64%), *MCL1* (30% vs 16%), *RB1* (25% vs 15%), *NKX2-1* (20% in both),

CDKN2A (16% vs 19%), *PIK3CA* (14% vs 17%), *MDM2* (14% vs 9%), and *CTNNB1* (7% vs 18%) also presented similar frequencies between the two cohorts. Of note, total 76/171 (44%) patients carried *TP53* DNA binding domain missense mutations (exons 4-8). However, co-drivers frequently found in advanced diseases, e.g. *BRAF* mutations, amplifications of *ERBB2,* or *MET* [13, 15, 26], were not as prevalent in our early-stage cohort.

We adopted the popular approach of testing DFS-based gene-by-treatment interaction effects to identify predictive genetic biomarkers for guiding treatment selection [22, 27]. We evaluated the predictive power of each mutated gene, and identified the following five predictive markers with significant treatment interactions (Table 1 and Methods): *RB1* alterations [interaction hazard ratio (iHR) 4.07, 95% confidence interval (CI) 1.56-10.58, *P*=0.004], *NKX2-1* CN gain [iHR 0.26 (95% CI 0.10-0.68), *P*=0.006], *CDK4* CN gain [iHR 0.14 (95% CI 0.03-0.77), *P*=0.024], *TP53* exon4/5 missense mutations [iHR 0.33 (95% CI 0.12-0.93), *P*=0.035], and *MYC* CN gain (iHR 0.10 (95% CI 0.01-0.98), *P*=0.048). Here, negative iHR indicated relative better survival with adjuvant TKI while positive iHR indicated relative benefit with adjuvant chemotherapy. Importantly, the treatment interactions remained significant for these five predictors even after adjusting for clinical parameters (Supplementary Table 2). The negative adjuvant TKI predictor, *RB1* alterations, combined *RB1* mutations and *RB1* CN loss, since they were functionally similar and both presented marginal significance of treatment interaction due to small sample size of each category (Supplementary Table 3). Besides, as missense mutations on different *TP53* exons might show distinct prognostic or predictive effects[28, 29], these exons were analyzed separately. Like RB1 alterations, both *TP53* exon 4 and 5 missense mutations (but not exons 6-8) showed marginal significance for treatment interactions and were therefore combined as a single predictive factor. Further, for prognostic analysis, we found that *TP53* exon4/5 missense mutations [multivariate HR 2.69 (95% CI 1.60-4.52), *P*<0.001] and *TP53* nonsense mutations [multivariate HR 1.69 (95% CI 1.08-2.65, *P*=0.022)] were both significantly correlated with worse outcomes irrespective of treatment arms, in concordance with *TP53* as a factor for negative prognosis (Supplementary Fig. 2, 3a, 3b). Other genetic aberrations that were significantly associated with prognosis were summarized in Supplementary Figure 3 and Supplementary Table 4.

Integrated MINERVA score via genomic signature

Each of the five biomarkers individually can predict the treatment outcomes for patient subgroups harboring each specific genetic alteration, although, a multigene signature integrating all mutational events at patient level is essential for estimating a patient's overall response to the molecular heterogeneity of early-stage NSCLC. We, therefore, constructed a MINERVA score to quantitatively assess individual tumors and their corresponding treatment responses by summing z scores from individual treatment-by-interaction test of the five selected genes. The resultant MINERVA scores of all the 171 tumors ranged from -7.09 to 2.88, including the 81 tumors (47.4%) that did not carry any alterations in the predictive genes (score=0) (Supplementary Fig. 4 and Methods). Based on the score distribution, we chose cutoffs between -0.5 and 0.5 to categorize the patients into three subgroups with lower score representing better response to adjuvant TKI. In the pre-categorized population, gefitinib significantly prolonged the median DFS, and increased the 2-year DFS rate, similar to the intention-to-treat (ITT) and

modified ITT populations[6] (Fig. 2a). Remarkably, after categorization by MINERVA, the three subgroups demonstrated distinct treatment responses and underlying molecular profiles (Fig. 2b, c). The Highly TKI-Preferable group [HTP, *N*=60, 35% (score≤-0.5)] expressed significant superiority with adjuvant gefitinib [HR 0.21 (95% CI 0.10-0.44)], and was enriched with copy number gain of *NKX2-1, CDK4* and *MYC*, and *TP53* exon 4/5 missense mutations. The TKI-Preferable group [TP, *N*=87, 51% (score -0.5 to 0.5)] showed improved DFS among the pre-categorized and ITT populations [HR 0.61 (95% CI 0.35-1.07)]. Besides, this subgroup was characterized by the absence of most predictive biomarkers, except for sporadic co-existence of *NKX2-1* and *RB1* alterations, with contrasting effects due to opposing iHRs (Table 1). Moreover, a small subset of patients, the Chemo-Preferable Group [CP, *N*=24, 14% (score≥0.5)], despite having *EGFR*-positive tumors, showed greater response and enhanced DFS [HR 3.06 (95% CI 0.99-9.53)] under VP treatment, and harbored *RB1* alterations (Fig. 2c).

In the TP group, the Kaplan-Meier estimate depicted similar curvatures as those observed in the pre-stratified and ITT populations [6] (Fig. 2a, e), indicating that adjuvant gefitinib achieved a superior DFS. Importantly, the survival curves of the post-categorized HTP and CP populations did not converge at any point (Fig. 2d, f). In HTP, the Kaplan-Meier curves separated widely as early as six months, with a slow descent of the adjuvant gefitinib arm (median DFS, 34.5 months; *P*<0.001). Conversely, a drastic drop of the VP arm towards a median DFS of 9.1 months was observed with all recurrence by 36 months. Therefore, the relative benefit of gefitinib was represented by a 6.4-fold increase in the 2-year DFS rate [70.3% (95% CI, 55.8-88.7) vs 11.0% (3.1-38.7)] and a 25.4-month longer median DFS (Fig. 2d). In the CP group, Kaplan-Meier curves diverged at 18 months with an immediate sharp decline of the gefitinib arm towards a median of 19.3 months. Meanwhile, 70% of the VP arm continued to benefit after 24 months (median DFS, 34.2 months, *P*=0.041). The superiority of adjuvant VP was reflected by a 1.7-fold increase in the 2-year DFS rate [69.2% (48.2-99.5)], including a 14.9-month longer median DFS, compared to the 41.6% 2-year DFS rate for gefitinib (95% CI 19.9-86.8) (Fig. 2f).

Stratification of OS benefit by MINERVA score

OS is generally considered as the standard endpoint for clinical trials. Although adjuvant gefitinib has shown significantly improved DFS relative to adjuvant VP, the DFS benefits in the ITT population did not translate into a significant difference in OS of the ADJUVANT trial [30], probably due to the combined influences of downstream treatment crossovers and the genetic heterogeneity among the patient population. Hence, we further used MINERVA in an attempt to achieve stratification of OS.

As expected, OS of the 171 pre-categorized patients involved in this study showed no difference between the two treatment groups (median, 76.9 months in the gefitinib group vs 67.1 months in the VP group; HR 0.87 (95% CI 0.57-1.35), *P*=0.54) (Fig. 3a and Supplementary Fig. 5). Promisingly, MINERVA successfully demonstrated the stratification of OS benefit as well. In HTP, gefitinib treatment led to significantly longer OS [median, not reached in the gefitinib group vs 48.7 months in the VP group; HR 0.43 (95% CI 0.21-0.88), *P*=0.018] with a clear and early separation of the Kaplan-Meier curves (Fig. 3b, c). Conversely, adjuvant VP treatment substantially improved OS in the CP group after 18 months [median, 36.4 months

in the gefitinib group vs not reached in the VP group; HR 2.47 (95% CI 0.76-8.02), *P*=0.12] (Fig. 3b, e). OS in TP mirrored that of the pre- categorized cohort, suggesting no differences between the treatments (Fig. 3a, d). Likewise, the 2-, 3- and 5-year survival rates of the categorized subgroups demonstrated similar trends, with the survival differences between the two treatments in both HTP and CP groups widened over time (Supplementary Fig. 6). The 5-year OS rates of gefitinib-treated HTP patients and VP-treated CP patients were 67.3% (95% CI 52.4-86.4) and 61.5% (95% CI 40.0-94.6), respectively, both of which were significantly higher than those attained in the pre-categorized cohort [gefitinib, 55.7% (95% CI 46.2-67.0); VP, 51.5% (95% CI 41.2-64.3)].

Internal validation of MINERVA score

We employed both ten-fold cross validation as well as LOOCV methods (as internal validation procedures) to evaluate the robustness of our MINERVA score. A relatively superior survival with adjuvant gefitinib treatment was observed in both HTP and TP subgroups, with an average of 3.5- and 1.9-fold increase in the 2-year DFS rate, respectively (Fig. 4a). The median DFS in these two subsets also increased by an average of 20 and 15 months, respectively (Fig. 4b), while the 2-year gefitinib-to-VP DFS ratio was less than 1, and the median DFS difference negative for all repeats in the CP group, suggesting greater survival benefit by adjuvant VP in this population. Among the 100 mock MINERVA score generated, 75% demonstrated significant treatment interaction with *P*-values <0.05, while 86% demonstrated interaction *P*-values <0.1 (Fig. 4c). We further validated the functionality of the original MINERVA score by LOOCV method. Adjuvant VP treatment in the HTP group was associated with markedly reduced DFS and OS (Fig. 4d, g). Meanwhile, adjuvant gefitinib treatment in the CP group was evidently inferior, similar to previously estimated results in Figures 2 and 3.

Discussion

To date, several prospective clinical trials, including our ADJUVANT trial, have presented the superiority of adjuvant TKI in early-stage *EGFR*-mutant NSCLC. The ADJUVANT trial had reached a median OS of 75.5 months by the database lock date, which is one of the best survival outcomes ever recorded for this patient population [31]. However, gefitinib's DFS superiority started declining after 36 months, and did not ultimately translate into OS benefit, raising concerns over achieving clinical cure by adjuvant TKI [32]. The heterogeneity in time-to-recurrence and OS observed within the ADJUVANT cohorts suggested high inter-tumor molecular heterogeneity in early-stage *EGFR*-mutant NSCLC [11], necessitating additional predictive biomarkers to redefine personalized adjuvant therapy.

In this first biomarker exploration of adjuvant TKI in resected NSCLC, we selected five genes that could independently predict the relative benefit between adjuvant TKI and chemotherapy. The multigene MINERVA score then integrated these biomarkers and effectively compensated for individuals' molecular heterogeneity. Notably, the three risk groups separated using this score counteracted the controversial impermanence of DFS benefit with exciting stratification of overall survival benefits as well. For each risk

groups, we also found characteristic enrichment of biomarkers, possibly explaining their differential responses to adjuvant treatments.

In the CP group, *RB1*-altered/*EGFR*-mutant patients showed better survival with adjuvant VP rather than gefitinib. In advanced NSCLC, TKI-resistant *RB1*-inactivated/*EGFR*-mutated adenocarcinoma clones have been found to transdifferentiate into small-cell lung cancer (SCLC) and become more responsive to chemotherapy[33, 34]. One of the potential mechanisms of SCLC transformation might be the disruption in expression of cell-state-determining factors due to *RB1* inactivation[16, 35]. The resulting lineage plasticity then converts the therapy-dependent cancer cells to those that express neuroendocrine lineage markers, making them refractory to targeted treatments[36, 37]. *RB1* often demonstrates mutual exclusivity with cell cycle pathway genes, and reflects chemosensitivity in rapidly progressing tumors [38], which is in line with our CP population. In hope to eradicate this subclone, researchers have developed an upfront trial in which patients with advanced stage were assigned to receive TKI and small-cell directed chemotherapy (platinum plus etoposide) alternately (NCT03567642). Further research is required to explore whether TKI insensitivity of RB1-inactive/EGFR-mutant patients in the adjuvant setting also arise from early histological transformation events.

Despite the small VP-favoring population, patients in the HTP subgroup presented significant benefits from adjuvant gefitinib therapy. Genomic analysis showed the enrichment of other four biomarkers, among which copy number gain of *NKX2-1* received nearly equal weightage as *RB1,* but in an opposite predictive direction that favors the choice of gefitinib. *NKX2-1* copy number gain is a widely prevalent oncogene found in up to 30% of *EGFR*-mutant patients [10]. *NKX2-1* amplification has been more frequently observed in TKI-treated patients with extended progression-free survival (≥24 months) [15]. These findings were consistent with its enrichment in the HTP population with relative gefitinib benefit. Previous studies mainly reported favorable prognosis with *NKX2-1* expression in mixed onco-driver, tumor stages and pathological backgrounds [39, 40], while our study is the first to demonstrate the predictive value of *NKX2-1* copy number gain to favor adjuvant TKI treatment in a more defined population.

TP53 as a tumor suppressor occurred in more than 50% of NSCLC, with mutations of complicated functional properties[17]. Unlike most tumor suppressor genes, missense mutations in the critical DNA binding domain (exons 4 to 8) are the most common variants in *TP53*, which are associated with the lower disease control rate and poorer survival outcomes with TKI treatment in contrast to *TP53* wildtypes in *EGFR*-mutant NSCLC[28, 41]. Apart from poor prognosis associated with loss-of-function *TP53* mutations, studies have also revealed varied prognostic effects of missense mutations on different *TP53* exons, suggesting possible functional divergence[29, 43, 44, 45, 46]. Interestingly, these missense variants could also be predictive for worse adjuvant chemotherapy outcomes compared to observation in resected NSCLC[42]. Along these lines, in this study, the predictive power of *TP53* variants was also assessed by exons. In the multigene model, the positive predictivity of *TP53* exons 4/5 missense mutations suggested that patients harboring these *TP53* mutations would relatively benefit more from gefitinib than VP. We did not consider exons 6-8 because they lacked predictive significance for adjuvant therapies under the treatment-

interaction test. In concert with the consensus on *TP53*'s negative prognostic effect, we did observe significantly lesser outcomes in *TP53*-positive patients despite the treatment they received.

Ideally, the development of a multi-gene clinical predictor requires a well-designed prospective validation with appropriate assumptions and sample size structured to address the underlying molecular heterogeneity. However, like most exploratory data analyses of clinical studies, our study lacked an external validation cohort. This challenge is unique in our case as there were no available equivalent public or clinical datasets of adjuvant TKI-treated patients with regular follow-up of survival outcome at the time of this study, and any prospective validation trials might span over another decade to reach maturity. Moreover, this score incorporated a relatively small training cohort, which may introduce biased biomarker selection, or an overfitted model. Therefore, it is important to exploit stringent statistical procedures to minimize cherry-picking during post hoc analyses. Cross-validating all the steps of model construction allowed us to evaluate whether the current algorithm could be uniformly applied to the entire cohort. Besides, only baseline specimen was examined in our study, while dynamic minimal residual disease (MRD) detection might provide additional information for the application of precise adjuvant TKI. However, consensus opinion on MRD's definition and detection technologies needed to be settled first.

Other limitations include insufficient tissue availability for retrospective genomic analysis of all the enrolled participants. However, both clinical characteristics and survival outcomes of the pre-categorized patients in this study were matched with those of the ITT population from the ADJUVANT trial.

Conclusions

The present exploratory retrospective analysis of the ADJUVANT trial unraveled the genetic constructs of *EGFR* co-mutations in stage II and III resected NSCLC. Further, the interplay between identified predictive markers and clinical outcomes was carefully examined, and incorporated into a multi-gene predictive score to aid the adjuvant paradigm. Our evidential MINERVA score presents a fresh perspective for future studies to examine its clinical validity, thereby guiding the development of more personalized adjuvant therapies, and their transition from bench to bedside.

Methods

Adjuvant Treated patients

All patients had Stage II-IIIA (N1-N2), *EGFR*-mutant NSCLC, underwent complete surgical resection and were randomized and treated in the ADJUVANT/CTONG1104 trial (NCT01405079) [6]. All except 27 patients initiated either adjuvant gefitinib or intravenous vinorelbine plus cisplatin between September 2011 and April 2014. All patients provided written informed consent for participating in ADJUVANT/CTONG1104 and this predefined biomarker study. *EGFR*-activating mutations were evaluated using amplification-refractory mutation system PCR at time of enrollment.

Clinical Efficacy Assessment

Per protocol, patients were assessed for disease-free survival by chest CT scan and abdominal ultrasound every 3 months, brain MRI every 6 months, bone scan every 12 months from baseline until disease relapse or death (whichever comes first) for up to 3 years. The survival after 3 years will be followed up semi-annually with telephone. Secondary endpoints, including overall survival, 3-year DFS rate, 5-year DFS rate, and 5-year OS rate, were also evaluated. Patients who were alive or lost to follow-up were censored on the last day they confirmed survival. The baseline demographics, clinical characteristics, and the primary end point data of ADJUVANT-CTONG1104, including the DFS, were collected from the previous publication [6]. Overall survival (OS) was updated either by phone interview, or on-site follow-up of the enrolled patients [30]. The study was approved by the research ethics boards of the participating hospitals, and was conducted in accordance with the ethical principles of the Declaration of Helsinki.

Sample details

Archived formalin-fixed paraffin-embedded (FFPE) tumor tissue specimens of 175 patients from the ADJUVANT/CTONG1104 trial were obtained from 25 centers (Figure 1). Only patients with sufficient and qualified tumor tissue samples who had been treated by either adjuvant arms were included in this study. Of these, a total of 171 patients positive for *EGFR* by NGS were subjected to further biomarker analyses (including 95 from the gefitinib group and 76 from the VP group).

DNA Extraction and Sequencing Library Preparation

Samples were sent to the CAP/CLIA (College of American Pathologists and Clinical Laboratory Improvements Amendments) accredited central laboratory at Nanjing Geneseeq Technology Inc. (Nanjing, China) for genomic DNA extraction and hybridization capture-based targeted NGS of 422 cancer-relevant genes. Protocols from previous publication were followed for both experimental procedures as well as sequence data analysis [48]. In detail, five to eight 10 μm FFPE sections were first de-paraffinized with xylene and then used for genomic DNA (gDNA) extraction by QIAamp DNA FFPE Tissue Kit (Qiagen) following the manufacturer's instructions. The extracted gDNA samples were quantified on Qubit 3.0 fluorometer (Thermo Fisher Scientific) and its purity was measured on Nanodrop 2000 (Thermo Fisher Scientific), following by fragmentation to a size around 350 bp by using Covaris M220 sonication system (Covaris) and then purified by size selection with Agencourt AMPure XP beads (Beckman Coulter).

Fragmented gDNA were used to prepare DNA libraries with KAPA hyper library preparation kit (KAPA Biosystems) according to the manufacturer's protocol. Libraries were then subjected to PCR amplification and purification with Agencourt AMPure XP beads before targeted enrichment.

Libraries with different sample indices were first pooled together to a total DNA amount of 2 μg and then subjected for targeted enrichment with IDT xGen Lockdown Reagents and a customized enrichment panel (Integrated DNA Technologies) covering the exonic regions of 422 genes and the introns of 16 fusion genes. The captured library was further amplified with Illumina p5 (5' AAT GAT ACG GCG ACC ACC GA 3') and p7 (5' CAA GCA GAA GAC GGC ATA CGA GAT 3') primers in KAPA Hifi HotStart ReadyMix

(KAPA Biosystems, Wilmington, MA) and purified with Agencourt AMPure XP beads. Sequencing libraries were quantified by qPCR with KAPA Library Quantification kit (KAPA Biosystems) and its size distribution was examined on Bioanalyzer 2100 (Agilent Technologies). The final libraries were sequenced on Illumina Hiseq 4000 platform for 150 bp paired-end sequencing according to the manufacturer's instructions. All experimental procedures were performed using validated assays.

Sequencing Data Analysis

Raw sequencing data was analyzed by a validated automation pipeline. In brief, raw data were first subjected to bcl2fastq for demultiplexing and then Trimmomatic[49] for FASTQ file quality control to remove low quality (base phred score below 30) and N bases. Reads were aligned to the reference human genome hg19 by Burrows-Wheller Aligner (BWA-mem, v0.7.12)[50]. PCR duplicates were removed by Picard. Genome Analysis Toolkit (GATK 3.4.0) was employed to apply the local realignment around indels and recalibrate base quality score. Single-nucleotide variations (SNVs) and insertion/deletion mutations were called using VarScan2 with the following parameters: 1) for mutations with more than 20 recurrences in COSMIC, minimum variant allele frequency (VAF) = 0.01 with at least 3 minimum variant supporting reads; 2) for others, minimum VAF = 0.02 with at least 5 minimum variant supporting reads; in addition, all variants also need to meet the standards of minimum read depth = 20, minimum base quality = 25, variant supporting reads mapped to both strands, and strand bias no greater than 10%.

CNV detection was using a self-developed pipeline, which has been validated in 38 samples against their droplet digital polymerase chain reaction (ddPCR) results as "gold standard". The system noise in copy number data was reduced by principal component analysis of 100 normal samples sequenced in the same batch.

Variant Filtering and Annotation

Single-nucleotide polymorphism (SNPs) and small insertions/deletions (indels) were annotated by ANNOVAR against the following databases: dbSNP (v138), 1000Genome, ExAC, COSMIC (v70), ClinVAR, and SIFT. Mutations that were presented in >1% population frequency in the 1000 Genomes Project or 65000 exomes project (ExAC) were removed. The resulted mutation lists were filtered through an internally collected list of recurrent sequencing errors on the same sequencing platform, which is summarized from the sequencing results of 200 normal samples with a minimum average sequencing depth of 700×. Specifically, if a variant was detected (i.e. ≥3 mutant reads and >1% VAF) in >20% of the normal samples, it was considered a likely artifact and was removed. Mutations occurred within the repeat masked regions were also removed.

Development of the MINERVA score

An interaction term, computed as a product of the biomarker and treatment variables, was incorporated in the Cox's proportional hazards regression[27] to identify predictive genomic alterations associated with improvement in relative DFS between adjuvant TKI and chemotherapy. Contrastingly, a treatment-

adjusted Cox's model, without the interaction term, was used to test for prognostic biomarkers. Subsequently, the gene-by-treatment interaction test was conducted for each gene feature separately, and a set of significant (P<0.05) features was selected. Relevant gene predictors were further tested (for interaction between treatment and each gene feature) through multivariate analysis, with the following clinical variables controlled: age, sex, smoking history, clinical stage, and lymph node stage (N stage).

We adapted a well-recognized linear discriminant model [25] to compile all predictive values of the potential predictive biomarkers into a composite MINERVA (Multiple-gene INdex to Evaluate the Relative benefit of Various Adjuvant therapies) score. The score for each patient was calculated using the following equation:

$$MINERVA_i = \sum_{g \in G} z_g p_{i,g},$$

where G is the set of selected genes g, z_g is the standardized test statistic of the interaction test for gene g, i is the i^{th} patient, while $p_{i,g}$ is the mutation status of g in the i^{th} patient.

Smaller values of MINERVA correspond to greater chance of benefiting from TKI than from chemotherapy as an adjuvant treatment. Based on the distribution of MINERVA scores, the patients could be effectively categorized into three subgroups with scores of <-0.5, -0.5 to 0.5, and >0.5, with distinct DFS outcomes. The relative survival benefit was compared using a 2-year DFS probability ratio and median DFS difference between gefitinib and VP arms [51].

Internal Validation of the MINERVA score

Ten-fold cross validation (CV) was used to evaluate the performance of our predictive model. In each iteration, interaction effect was assessed by cox proportional hazard model based on 90% of the samples. An identical modeling procedure as described above was performed for genetic marker selection and model construction. Mock MINERVA scores were then calculated for the remaining 10% samples based on the model developed in the training samples. A complete set of scores can be computed through ten repeated 10-fold CV and patients were assigned to one of the three MINERVA subgroups accordingly (HTP <-0.5, TP -0.5~0.5, or CP >0.5). Predictive effect of the mock MINERVA scores was then evaluated with interaction p-value. This process was repeated 100 times. Relative adjuvant treatment benefit within each subgroup was compared using 2-year disease-free survival probability and median disease-free survival difference between gefitinib and VP arms.

Next, we performed leave-one-out cross validation (LOOCV) to obtain individual scores. Each patient was omitted in alternation and then scored by MINERVA constructed on the remaining 170 patients (including both gene marker selection and model construction). The patient was then assigned to one of subgroups with the same score cutoffs. The entire procedure was repeated until each patient was left out once, scored and grouped. Kaplan-Meier curves were estimated for each subgroup to evaluate relative benefit

of adjuvant gefitinib to VP therapy using 2-year disease-free survival ratio, median disease-free survival difference and the log-rank p values.

Statistical analysis

Univariate and multivariate analyses of the association of biomarkers, treatment interaction, and clinical factors with DFS were performed with the Cox proportional hazard regression model. Kaplan-Meier curves of DFS and OS were estimated for each subgroup, and statistically compared using the log-rank test. A two-sided *P*-value <0.5 was considered statistically significant. All statistical analyses were performed using R software (version 3.5.0).

Declarations

ACKNOWLEDGEMENTS

We thank the patients and their families, staff members at all study sites, and investigators from CTONG for their help with this study. The study was supported by the Chinese Thoracic Oncology Group (CTONG) and the following grants: Key Lab System Project of Guangdong Science and Technology Department - Guangdong Provincial Key Lab of Translational Medicine in Lung Cancer (Grant No. 2017B030314120, to Prof. Yi-Long Wu), National Natural Science Foundation of China (Grant No.81872510, to Prof. Wen-Zhao Zhong), and Guangdong Provincial People's Hospital Intermural Program (Grant No. DFJH201917, to Dr. Si-Yang Liu).

AUTHOR CONTRIBUTIONS

S-YL and Y-LW designed the study. S-YL, QW, W-MM, LW, CC, YiC and W-ZZ collected data. S-YL, HB, YeC, XT and H-HY designed methodology and performed data interpretation. S-YL, HB, YeC, and XT prepared the manuscript. SD, X-CZ, JS, J-JY, X-NY, QZ, XW, YS, W-ZZ and Y-LW reviewed and revised the manuscript. All authors discussed results and contributed to the finalization of the manuscript.

DECLARATION OF INTERESTS

LW declares speaker fees from AstraZeneca, Eli Lilly, Pfizer, Roche, and Sanofi. W-ZZ declares speaker fees from AstraZeneca and Roche. Y-LW reports consulting and advisory services and declares speaker fees for Roche, AstraZeneca, Eli Lilly, Boehringer Ingelheim, Sanofi, MSD and BMS. HB, YeC, XT, XW, and YS are employees of Geneseeq Technology Inc., Nanjing, China. All other authors declare no conflict of interest.

References

1. Winton T*, et al.* Vinorelbine plus cisplatin vs. observation in resected non-small-cell lung cancer. *N Engl J Med* **352**, 2589-2597 (2005).

2. Arriagada R*, et al.* Long-term results of the international adjuvant lung cancer trial evaluating adjuvant Cisplatin-based chemotherapy in resected lung cancer. *J Clin Oncol* **28**, 35-42 (2010).

3. Pignon JP*, et al.* Lung adjuvant cisplatin evaluation: a pooled analysis by the LACE Collaborative Group. *J Clin Oncol* **26**, 3552-3559 (2008).

4. Kelly K*, et al.* Adjuvant Erlotinib Versus Placebo in Patients With Stage IB-IIIA Non-Small-Cell Lung Cancer (RADIANT): A Randomized, Double-Blind, Phase III Trial. *J Clin Oncol* **33**, 4007-4014 (2015).

5. Goss GD*, et al.* Gefitinib versus placebo in completely resected non-small-cell lung cancer: results of the NCIC CTG BR19 study.

6. Zhong W-Z*, et al.* Gefitinib versus vinorelbine plus cisplatin as adjuvant treatment for stage II–IIIA (N1–N2) EGFR -mutant NSCLC (ADJUVANT/CTONG1104): a randomised, open-label, phase 3 study. *The Lancet Oncology* **19**, 139-148 (2018).

7. Yue D*, et al.* Erlotinib versus vinorelbine plus cisplatin as adjuvant therapy in Chinese patients with stage IIIA EGFR mutation-positive non-small-cell lung cancer (EVAN): a randomised, open-label, phase 2 trial. *The Lancet Respiratory Medicine*, (2018).

8. Pennell NA*, et al.* SELECT: A Phase II Trial of Adjuvant Erlotinib in Patients With Resected Epidermal Growth Factor Receptor-Mutant Non-Small-Cell Lung Cancer. *Journal of clinical oncology : official journal of the American Society of Clinical Oncology* **37**, 97-104 (2019).

9. Wu Y-L*, et al.* Osimertinib in Resected EGFR-Mutated Non–Small-Cell Lung Cancer. *New England Journal of Medicine*, (2020).

10. Skoulidis F, Heymach JV. Co-occurring genomic alterations in non-small-cell lung cancer biology and therapy. *Nat Rev Cancer* **19**, 495-509 (2019).

11. Jamal-Hanjani M*, et al.* Tracking the Evolution of Non-Small-Cell Lung Cancer. *N Engl J Med* **376**, 2109-2121 (2017).

12. McGranahan N, Favero F, Bruin ECd, Birkbak NJ, Szallasi Z, Swanton C. Clonal status of actionable driver events and the timing of mutational processes in cancer evolution. *Sci Transl Med* **7**, 283ra254 (2015).

13. Blakely CM*, et al.* Evolution and clinical impact of co-occurring genetic alterations in advanced-stage EGFR-mutant lung cancers. *Nat Genet* **49**, 1693-1704 (2017).

14. Nahar R*, et al.* Elucidating the genomic architecture of Asian EGFR-mutant lung adenocarcinoma through multi-region exome sequencing. *Nat Commun* **9**, 216 (2018).

15. Chen M*, et al.* Concurrent Driver Gene Mutations as Negative Predictive Factors in Epidermal Growth Factor Receptor-Positive Non-Small Cell Lung Cancer. *EBioMedicine* **42**, 304-310 (2019).

16. Offin M*, et al.* Concurrent RB1 and TP53 Alterations Define a Subset of EGFR-Mutant Lung Cancers at risk for Histologic Transformation and Inferior Clinical Outcomes. *Journal of Thoracic Oncology* **14**, 1784-1793 (2019).

17. Canale M*, et al.* Impact of TP53 Mutations on Outcome in EGFR-Mutated Patients Treated with First-Line Tyrosine Kinase Inhibitors. *Clinical Cancer Research: An Official Journal of the American Association for Cancer Research* **23**, 2195-2202 (2017).

18. Voss MH*, et al.* Genomically annotated risk model for advanced renal-cell carcinoma: a retrospective cohort study. *The Lancet Oncology* **19**, 1688-1698 (2018).

19. Paik S*, et al.* A Multigene Assay to Predict Recurrence of Tamoxifen-Treated, Node-Negative Breast Cancer. *N Engl J Med* **351**, 2817-2826 (2004).

20. Ballman KV. Biomarker: Predictive or Prognostic? *J Clin Oncol* **33**, 3968-3971 (2015).

21. Andersson J*, et al.* Worse survival for TP53 (p53)-mutated breast cancer patients receiving adjuvant CMF. *Ann Oncol* **16**, 743-748 (2005).

22. Rothwell PM. Subgroup analysis in randomised controlled trials. *Lancet* **365**, 176–186 (2005).

23. Brugger W*, et al.* Prospective molecular marker analyses of EGFR and KRAS from a randomized, placebo-controlled study of erlotinib maintenance therapy in advanced non-small-cell lung cancer. *J Clin Oncol* **29**, 4113-4120 (2011).

24. Perez EA*, et al.* Genomic analysis reveals that immune function genes are strongly linked to clinical outcome in the North Central Cancer Treatment Group n9831 Adjuvant Trastuzumab Trial. *J Clin Oncol* **33**, 701-708 (2015).

25. Matsui S, Simon R, Qu P, Shaughnessy JD, Jr., Barlogie B, Crowley J. Developing and validating continuous genomic signatures in randomized clinical trials for predictive medicine. *Clin Cancer Res* **18**, 6065-6073 (2012).

26. Yu HA*, et al.* Concurrent Alterations in EGFR-Mutant Lung Cancers Associated with Resistance to EGFR Kinase Inhibitors and Characterization of MTOR as a Mediator of Resistance. *Clin Cancer Res* **24**, 3108-3118 (2018).

27. Ternes N, Rotolo F, Michiels S. Robust estimation of the expected survival probabilities from high-dimensional Cox models with biomarker-by-treatment interactions in randomized clinical trials. *BMC*

Med Res Methodol **17**, 83 (2017).

28. Canale M*, et al.* Impact of TP53 Mutations on Outcome in EGFR-Mutated Patients Treated with First-Line Tyrosine Kinase Inhibitors. *Clin Cancer Res* **23**, 2195-2202 (2017).

29. Vega FJ*, et al.* p53 exon 5 mutations as a prognostic indicator of shortened survival in non-small-cell lung cancer. *Br J Cancer* **76**, 44-51 (1997).

30. Zhong WZ*, et al.* Gefitinib Versus Vinorelbine Plus Cisplatin as Adjuvant Treatment for Stage II-IIIA (N1-N2) EGFR-Mutant NSCLC: Final Overall Survival Analysis of CTONG1104 Phase III Trial. *J Clin Oncol*, JCO2001820 (2020).

31. Goldstraw P*, et al.* The IASLC Lung Cancer Staging Project: Proposals for Revision of the TNM Stage Groupings in the Forthcoming (Eighth) Edition of the TNM Classification for Lung Cancer. *J Thoracic Oncol* **1**, 39-51 (2016).

32. Ng TL, Camidge DR. Lung cancer's real adjuvant EGFR targeted therapy questions. *The Lancet Oncology* **19**, 15-17 (2018).

33. Niederst MJ*, et al.* RB loss in resistant EGFR mutant lung adenocarcinomas that transform to small-cell lung cancer. *Nat Commun* **6**, 6377 (2015).

34. Lee J-K*, et al.* Clonal History and Genetic Predictors of Transformation Into Small-Cell Carcinomas From Lung Adenocarcinomas. *J Clin Oncol* **35**, 3065-3074 (2017).

35. Walter DM*, et al.* RB constrains lineage fidelity and multiple stages of tumour progression and metastasis. *Nature* **569**, 423-427 (2019).

36. Ku SY*, et al.* Rb1 and Trp53 cooperate to suppress prostate cancer lineage plasticity, metastasis, and antiandrogen resistance. *Science* **355**, 78-83 (2017).

37. Marcoux N*, et al.* EGFR-Mutant Adenocarcinomas That Transform to Small-Cell Lung Cancer and Other Neuroendocrine Carcinomas: Clinical Outcomes. *Journal of Clinical Oncology* **37**, 278-285 (2019).

38. Knudsen ES, Pruitt SC, Hershberger PA, Witkiewicz AK, Goodrich DW. Cell Cycle and Beyond: Exploiting New RB1 Controlled Mechanisms for Cancer Therapy. *Trends Cancer* **5**, 308-324 (2019).

39. Li X*, et al.* Thyroid transcription factor-1 amplification and expressions in lung adenocarcinoma tissues and pleural effusions predict patient survival and prognosis. *Journal of thoracic oncology : official publication of the International Association for the Study of Lung Cancer* **7**, 76-84 (2012).

40. Anagnostou VK, Syrigos KN, Bepler G, Homer RJ, Rimm DL. Thyroid transcription factor 1 is an independent prognostic factor for patients with stage I lung adenocarcinoma. *J Clin Oncol* **27**, 271-278 (2009).

41. Wei Y*, et al.* Three new disease-progression modes in NSCLC patients after EGFR-TKI treatment by next-generation sequencing analysis. *Lung Cancer* **125**, 43-50 (2018).

42. Ma X*, et al.* Significance of TP53 mutations as predictive markers of adjuvant cisplatin-based chemotherapy in completely resected non-small-cell lung cancer. *Mol Oncol* **8**, 555-564 (2014).

43. Shepherd FA*, et al.* Pooled Analysis of the Prognostic and Predictive Effects of TP53 KRAS. *Journal of Clinical Oncology* **35**, 2018-2027 (2017).

44. Li XM*, et al.* Predictive and Prognostic Potential of TP53 in Patients With Advanced Non-Small-Cell Lung Cancer Treated With EGFR-TKI: Analysis of a Phase III Randomized Clinical Trial (CTONG

0901). *Clin Lung Cancer* **22**, 100-109 e103 (2021).

45. Liu Y*, et al.* Mutations in exon 8 of TP53 are associated with shorter survival in patients with advanced lung cancer. *Oncol Lett* **18**, 3159-3169 (2019).

46. Li X*, et al.* P3.01-067 TP53 Mutations Could Involve in EGFR-TKI Primary Resistance in Advanced Non-Small Cell Lung Cancer. *Journal of Thoracic Oncology* **12**, S2227 (2017).

47. Labbe C*, et al.* Prognostic and predictive effects of TP53 co-mutation in patients with EGFR-mutated non-small cell lung cancer (NSCLC). *Lung Cancer* **111**, 23-29 (2017).

48. Yang Z*, et al.* Investigating Novel Resistance Mechanisms to Third-Generation EGFR Tyrosine Kinase Inhibitor Osimertinib in Non-Small Cell Lung Cancer Patients. *Clinical cancer research : an official journal of the American Association for Cancer Research* **24**, 3097-3107 (2018).

49. Bolger AM, Lohse M, Usadel B. Trimmomatic: a flexible trimmer for Illumina sequence data. *Bioinformatics* **30**, 2114-2120 (2014).

50. Li H, Durbin R. Fast and accurate short read alignment with Burrows-Wheeler transform. *Bioinformatics* **25**, 1754-1760 (2009).

51. Iasonos A, Chapman PB, Satagopan JM. Quantifying Treatment Benefit in Molecular Subgroups to Assess a Predictive Biomarker. *Clin Cancer Res* **22**, 2114-2120 (2016).

Table

Table 1. Predictive Values of Different Genomic Aberrations Derived according to Disease-free Survival (DFS)

Predictive markers (treatment-by-gene interaction)				
Mutation Subgroup	**Recurrence Events/ No. of Patients**	**iHR[a] (95% CI[b])**	**z-score**	***P* Value**
RB1 alterations	23/33	4.07 (1.56-10.58)	2.88	0.004
NKX2-1 CN[c] gain	23/34	0.26 (0.10-0.68)	-2.72	0.006
CDK4 CN[c] gain	7/12	0.14 (0.03-0.77)	-2.26	0.024
TP53 exon4/5 missense mutations	20/29	0.33 (0.12-0.93)	-2.11	0.035
MYC CN[c] gain	7/15	0.10 (0.01-0.98)	-1.98	0.048

[a] iHR, interaction hazard ratio between treatments and gene alterations;

[b] CI, confidence interval;

[c] CN, copy number.

Figures

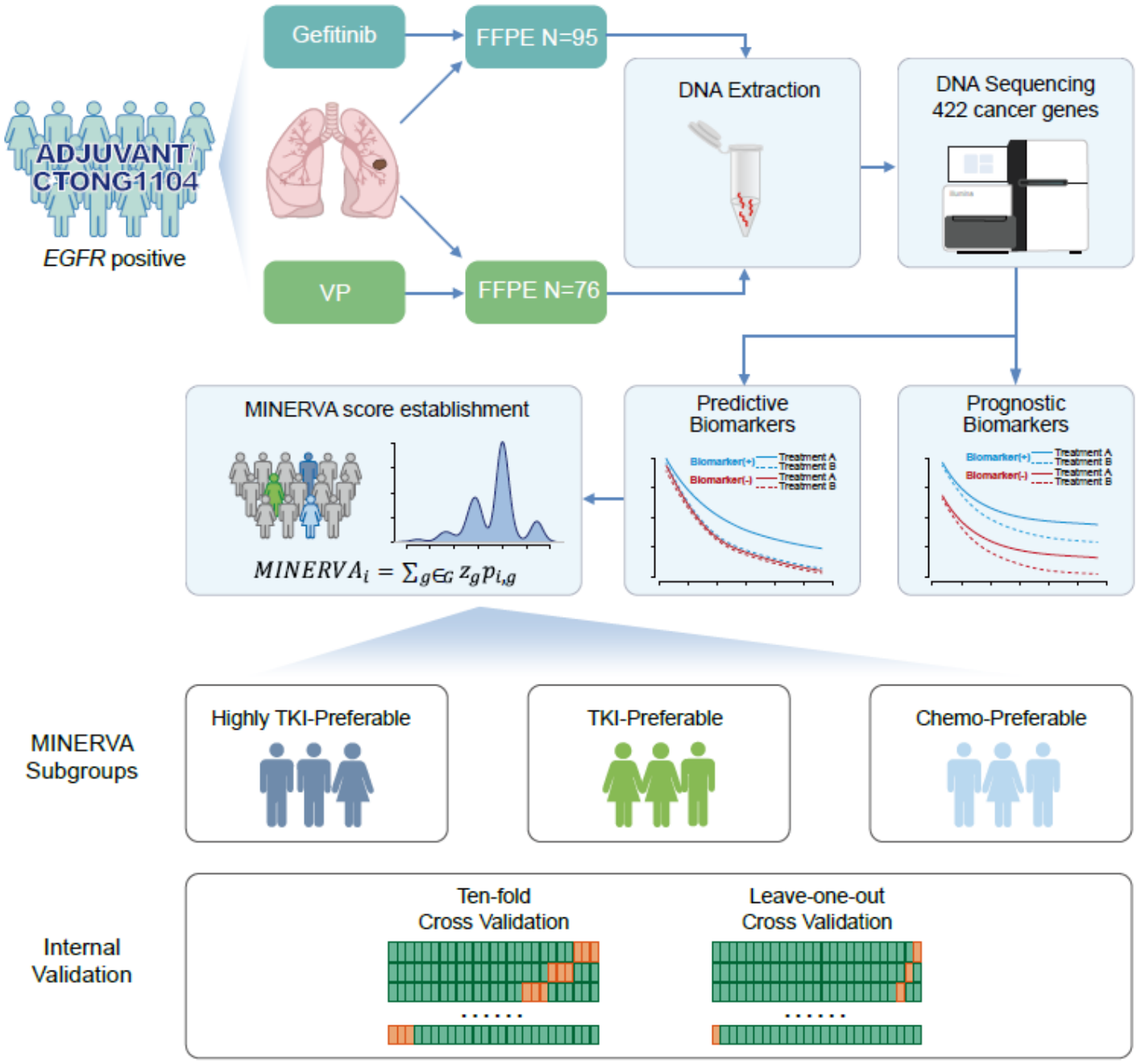

Figure 1

Schematic Diagram of Patient Screening, Sample Collection, and Methodology for Developing the Clinical Predictive Model

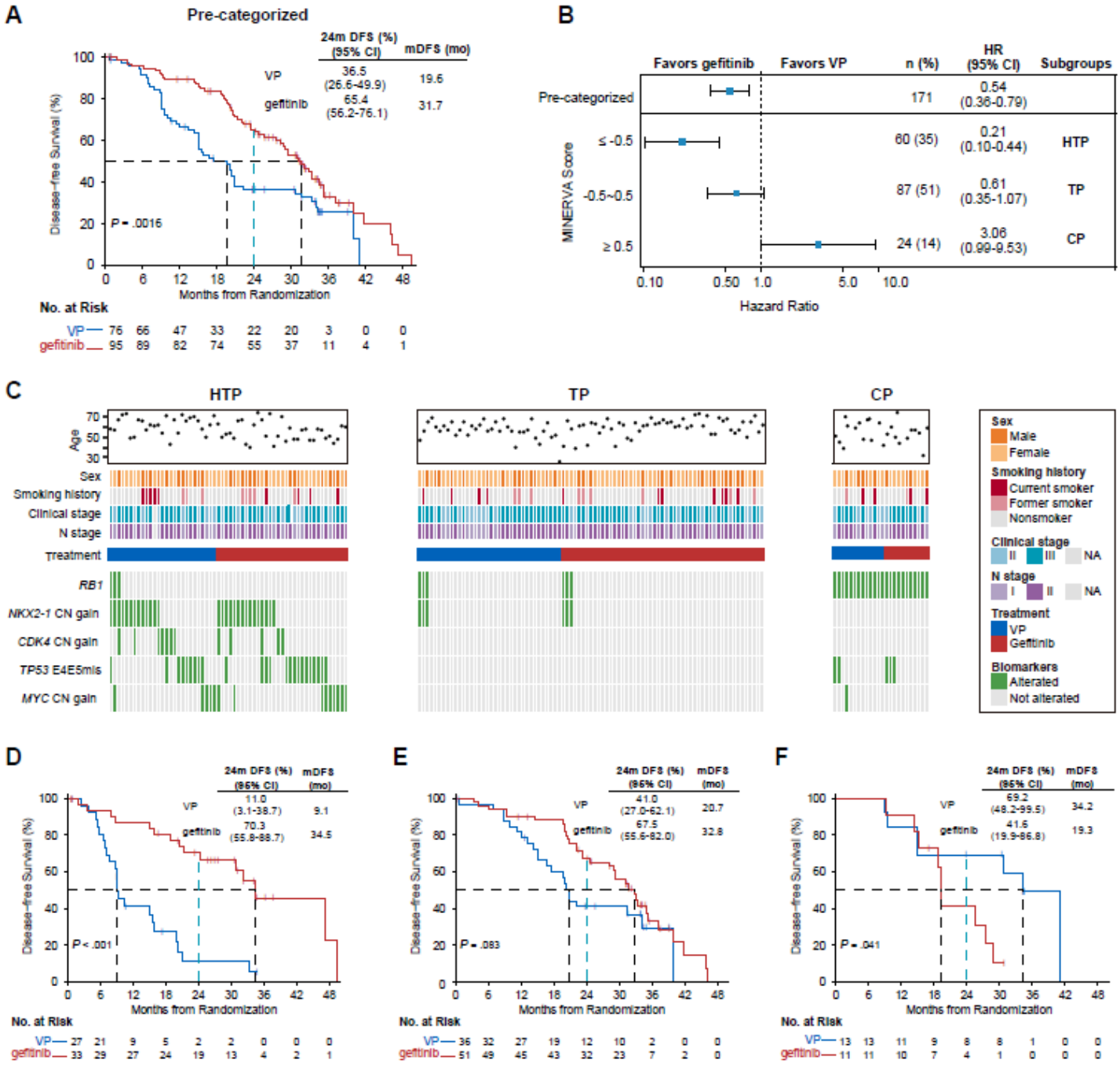

Figure 2

Disease-free Survival (DFS) as per MINERVA subgroups. a Kaplan-Meier curves estimate DFS of the pre-categorized cohort which received adjuvant gefitinib or VP treatment (N=171). b Forest plot showing the hazard ratio (HR) of DFS in subgroups (HTP, highly TKI-preferable group; TP, TKI-preferable group; CP, chemo-preferable group) classified by MINERVA score. Error bars indicate 95% CIs. c-e Kaplan-Meier curves of DFS for patients treated by adjuvant gefitinib or VP in three MINERVA subgroups. Black dotted lines indicate median DFS. Blue doted lines indicate 2-year survival rates (24 months). P values were derived from the log-rank test.

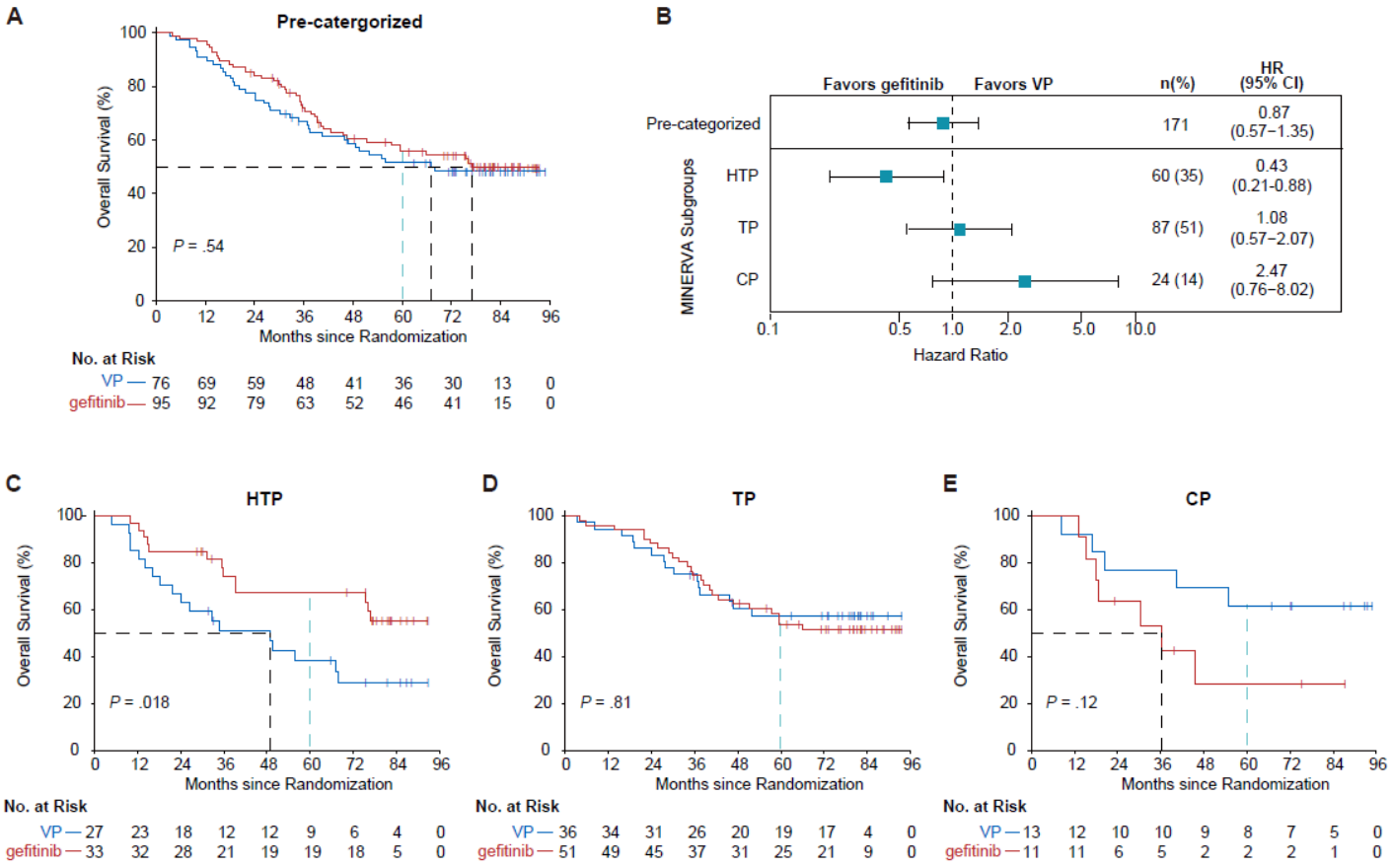

Figure 3

Updated overall survival (OS) and OS benefit stratification by MINERVA. a Kaplan-Meier curves of OS for the intention-to-treat (ITT) population (N=222) who received adjuvant gefitinib or VP treatment in the original ADJUVANT trial. b Annual survival rates for the ITT population who received adjuvant gefitinib or VP treatment. Error bars indicate 95% confidence intervals (CIs). c Kaplan-Meier estimates of OS for the pre-stratified cohort included in this study (N=171). d Forest plot showing hazard ratio (HR) of OS in MINERVA subgroups. Error bars indicate 95% CI. e-g Kaplan-Meier curves estimate OS in each subgroup by treatments. Dotted lines in black indicate median overall survival. Dotted lines in blue indicate 5-year survival rate (60 months). P values were derived from the log-rank test.

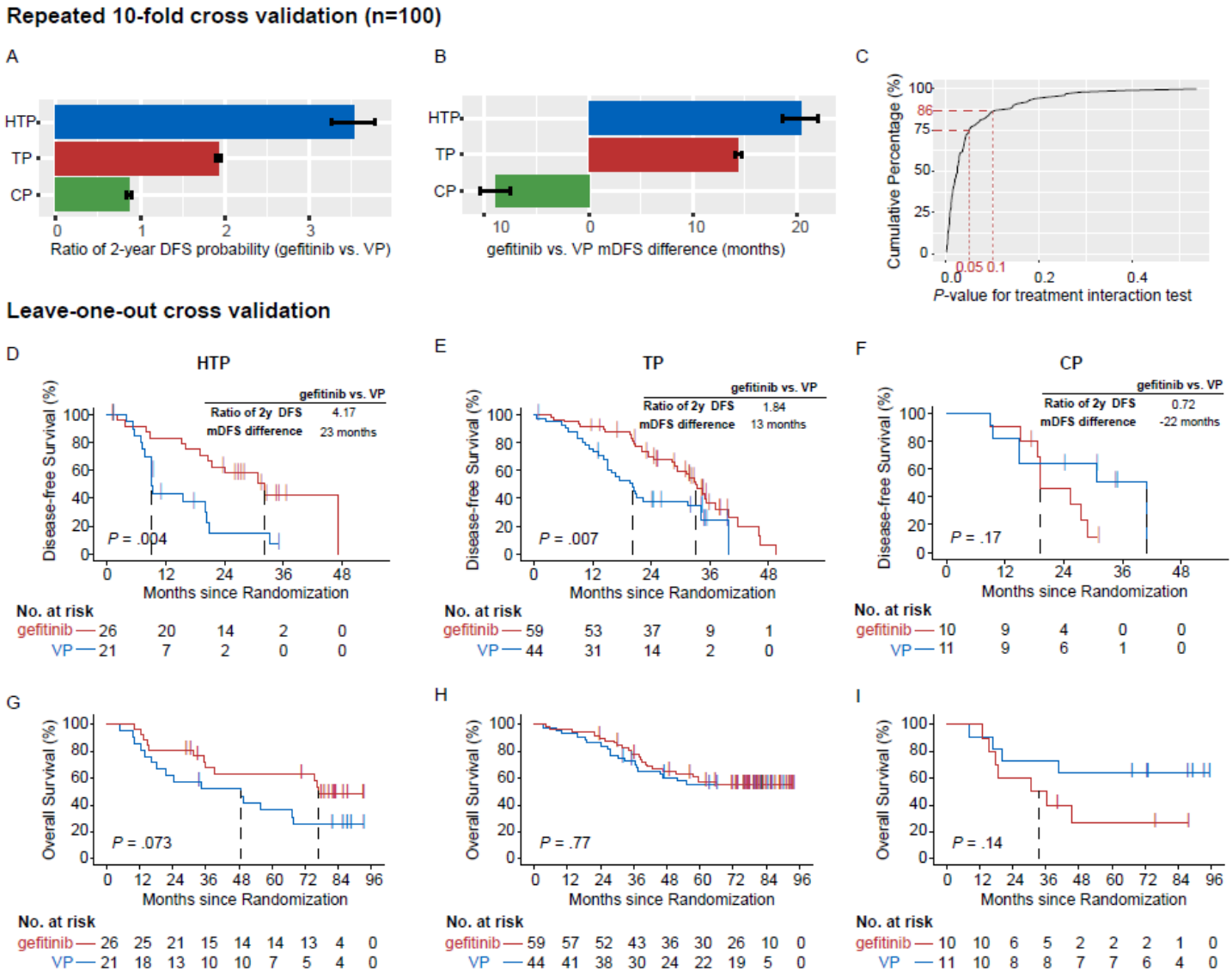

Figure 4

Internal validation of MINERVA. a-b Ten-fold cross validation was repeated 100 times to assess relative benefit among three MINERVA risk groups by (a) ratio of 2-year disease-free survival (DFS) probability comparing gefitinib to VP, and (b) difference in median DFS between gefitinib and VP treated patients. Error bars indicate standard error from 100 repeats. c Curve showing the cumulative percentage of mock MINERVA models from 100 repeated 10-fold cross validation and corresponding p-values derived from the MINERVA-by-treatment interaction tests. Red dotted lines indicate percentage of repeats with interaction P <0.05 or <0.1. d-f Kaplan-Meier estimates of DFS in three mock MINERVA subgroups derived by leave-one-out cross validation. g-i Kaplan-Meier estimates of OS in three mock MINERVA subgroups.

Supplementary Files

This is a list of supplementary files associated with this preprint. Click to download.

- 20210413NCSupplementaryV2.docx